This article has been accepted for publication in a future issue of this journal, but has not been fully edited. Content may change prior to final publication. Citation information: DOI 10.1109/LSP.2017.2737596, IEEE Signal Processing Letters

Chirp Spread Spectrum towards the Nyquist Signaling Rate — Orthogonality Condition and Applications

Xing Ouyang, Octavia A. Dobre, Yong Liang Guan and Jian Zhao

***Abstract*—With the proliferation of Internet-of-Things (IoT), the chirp spread spectrum (CSS) technique is re-emerging for communications. Although the chirps can offer high processing gain, its poor spectral efficiency and the lack of orthogonality among different chirps tend to limit its potential. In this paper, we derive the condition to orthogonally multiplex an arbitrary number of linear chirps. For the first time in the literature, we show that the maximum modulation rate of the linear chirps satisfying the orthogonality condition can approach the Nyquist signaling rate, the same as single-carrier waveforms with Nyquist signaling or orthogonal frequency-division multiplexing signals. The performance of the proposed orthogonal CSS is analyzed in comparison to the emerging LoRa™ systems for IoT applications with power constraint, and its capability for high-speed communications is also demonstrated in the sense of Nyquist signaling.**

***Index Terms*—Chirp spread spectrum (CSS); Nyquist waveform; Fresnel transform; orthogonal chirp-division multiplexing (OCDM); Internet-of-Things (IoT).**

I. Introduction

THE chirp is a special class of frequency-modulated waveforms that is well known for being widely adopted in radar systems. For communications, the chirp spread spectrum (CSS) has been considered in the ultra-wideband systems, as specified in the IEEE 802.15.4a standard [1], and in the emerging Semtech's LoRa™ systems for low-power wide area network (LPWAN) [2-4]. In particular, with the proliferation of Internet-of-Things (IoT) and machine-to-machine communications, the LoRa-CSS scheme provides a unique solution to address the demand for low-power, long-range and low-cost communications, leading to the re-emergence of the CSS technique, along with intensive research interest and activities.

The unique properties of the chirped signals, namely spread spectrum and pulse compression promise reliable communications of low-power consumption over long distance, robustness against interference and noise in hostile environments, and insensitivity to time and frequency offsets caused by the imperfections of electronics in transceivers or by high mobility [5-7]. However, the CSS technique exhibits a poor spectral efficiency, resulting from the loss of orthogonality among different chirped waveforms. If more than one chirp is used within the same time period and bandwidth, interference arises from the non-orthogonality, and thus the modulation rate of the chirped waveforms is far from the Nyquist rate.

In the literature, there are works on CSS systems that deal with a balance between the processing gain and data rate, rather than focusing on the orthogonality itself. For example, in [8], using frequency-division multiplexing, the processing gain is sacrificed for higher spectral efficiency and vice versa. In the LoRa-CSS, frequency-shift keying (FSK) is adopted to improve the spectral efficiency. However, the maximum data rate is 37.5 kbps with a minimum 25% forward error correction (FEC) overhead over 500 kHz bandwidth in the 868 MHz ISM-band [9]. Moreover, it is proved in [10] that the orthogonality does not hold among the chirps. Performance degradation thus occurs compared to the traditional FSK system, and should be compensated by using a higher processing gain or coding gain.

Notably, by utilizing the discrete Fresnel transform (DFnT), orthogonal chirp-division multiplexing (OCDM) is proposed in [11-14] for high-speed communication at the Nyquist rate. It is proved that orthogonality holds among the chirps in the discrete-time domain. However, in the continuous-time domain, the orthogonality is destroyed, which agrees with the result in [10]. In addition, in the discrete-time OCDM system, the processing gain of the chirps equals the time-bandwidth product of the signal. It means that for a given bandwidth, once the processing gain is fixed, the number of discrete-time chirps is fixed for information multiplexing. This constraint makes the design of a CSS system inflexible for various applications.

In this letter, we theoretically prove the orthogonality condition for the CSS system in the analog domain. Based on this condition, it is shown that the modulation rate of the linear chirps can approach the Nyquist rate, same as the single-carrier and orthogonal frequency division multiplexing (OFDM) systems. It is also shown that it is possible to synthesize an arbitrary number of continuous-time chirps, whose processing gain can be arbitrarily chosen without the constraint in the OCDM system [11-14]. It means that the design of the orthogonal CSS in this letter is more flexible to meet the requirements of different applications, while preserving the orthogonality in ana-

Xing Ouyang and Jian Zhao are with the Tyndall National Institute and also the School of Electrical and Electronic Engineering, University College Cork, Cork, T12C5CP, Ireland.

Octavia A. Dobre is the Faculty of Engineering and Applied Science, Memorial University, St. John's, NL A1B 3X5, Canada.

Yong Liang Guan is with the School of Electrical and Electronic Engineering, Nanyang Technological University, Singapore.

This article has been accepted for publication in a future issue of this journal, but has not been fully edited. Content may change prior to final publication. Citation information: DOI 10.1109/LSP.2017.2737596, IEEE Signal Processing Letters

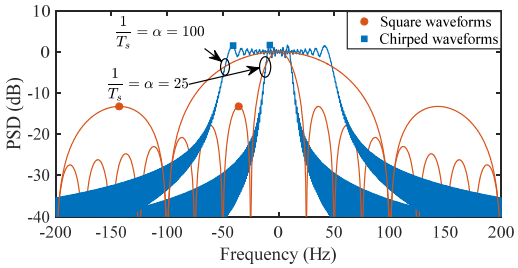

Fig. 1. The PSD functions of chirped-waveforms of period $T = 1$ s and chirp rates $\alpha = 25$ and 100 Hz^2, and square waveforms with periods $T_s = 0.04$ and 0.01 second (25 and 100 Hz), respectively.

log domain. We also show that the orthogonal CSS is able to, for its capability of Nyquist signaling and spread-spectrum, fulfill the purposes of power-limited systems, such as LPWAN, and also high-speed communications by employing modulation formats such as quadrature amplitude modulation (QAM).

II. Chirp Spread Spectrum: Preliminaries

A linearly chirped waveform, with chirp rate α and period T, has a constant amplitude and linearly modulated frequency, as

$$\psi(t) = \frac{1}{\sqrt{T}} e^{j\pi\alpha t^2}, \quad -\frac{T}{2} \le t < \frac{T}{2}. \tag{1}$$

The spectrum of the chirp can be obtained using the Fourier transform, and with some mathematical manipulations it can be given in terms of the Fresnel integral [Chapter 7.3, 15] as

$$\begin{aligned}\psi_\Omega(f) &= \mathcal{F}_\Omega\{\psi(t)\} = \frac{1}{\sqrt{T}}\int_{-T/2}^{+T/2} e^{j\pi\alpha t^2} e^{j2\pi ft}\,\mathrm{d}t \\ &= \frac{1}{\sqrt{\alpha}} e^{j\frac{\pi}{\alpha}f^2}\left[F_\Psi\left(\frac{f}{\sqrt{\alpha}} + \sqrt{\alpha}\frac{T}{2}\right) - F_\Psi\left(\frac{f}{\sqrt{\alpha}} - \sqrt{\alpha}\frac{T}{2}\right)\right],\end{aligned} \tag{2}$$

where $F_\Psi(x)$ is the complex Fresnel integral, defined as

$$F_\Psi(x) = \int_0^x e^{-j\pi t^2}\,\mathrm{d}t\,. \tag{3}$$

Fig. 1 illustrates the power spectral density (PSD) functions of chirps with period $T = 1$ s and chirp rates $\alpha = 25$ and 100 Hz^2, respectively. For comparison, the PSD functions of the square waveforms with periods of $T_s = 0.04$ and 0.01s are provided for comparison. It can be seen that although their PSDs have quite different shapes, both occupy similar bandwidth if $\alpha T \approx 1/T_s$.

According to the Nyquist-Shannon criterion, within a given bandwidth B Hz, the maximum degree-of-freedom of a waveform available for modulation is B Baud/s. For instance, using the squared-waveforms and arranging the sinc-like subcarriers in the frequency domain, OFDM attains the Nyquist rate if the number of subcarriers is large enough. Similarly, single-carrier systems with the sinc-waveforms approach the Nyquist rate in the time domain. To date, in the CSS systems, chirped waveforms are unable to achieve the Nyquist rate as there is no chirp which meets the orthogonality condition for Nyquist signaling.

III. Orthogonality Condition for CSS

In this section, we first introduce the Talbot effect, an optical phenomenon from the periodic repetition of Fresnel diffraction,

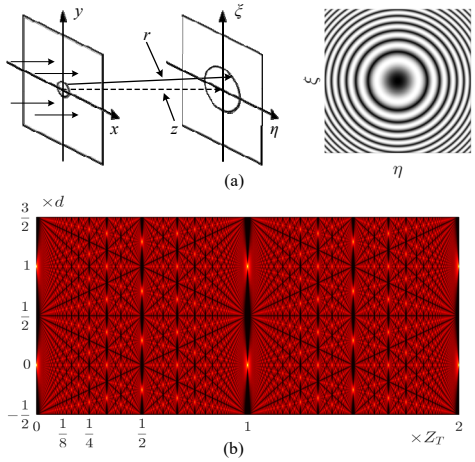

Fig. 2. Illustrations of (a) the Fresnel diffraction whose spatial phase quadratically increases from the origin, and (b) the Talbot effect that is the infinitely extended Fresnel diffraction with period d, and in which at a fractional Talbot distance Z_T / N, there are N duplicate images of the one at the origin.

as depicted in Fig. 2 [16]. The orthogonality condition for the chirped waveform to achieve Nyquist signaling is derived in analogy to the critical condition of the Talbot effect.

A. Talbot Effect and the Orthogonality Condition

As shown in Fig. 2 (a), the diffraction pattern of a Fresnel diffraction on the right plane is given by [17]

$$f_\Psi(\eta) = \frac{1}{\sqrt{a}} e^{j\frac{\pi}{4}} \times \int f(x) e^{j\frac{\pi}{a}(\eta - x)^2}\,\mathrm{d}x\,, \tag{4}$$

where $f(x)$ is the transfer function of the aperture with respect to the x-axis, and $a = \lambda z$ is the spatial coefficient with λ as the wavelength and z as the distance between the planes. It can be observed that the phase of the Fresnel diffraction in Fig. 2 (a) is quadratic along the radius from the origin, and the spatial frequency is linear. Comparing the spatial coefficient a and the chirp rate α in (1), we have $a = 1/\alpha$.

The Talbot image in Fig. 2 (b) is obtained by infinitely extending the Fresnel diffraction with periodicity d. It can be seen that at $z = Z_T$, with Z_T being the Talbot distance

$$Z_T = d^2/\lambda\,, \tag{5}$$

the duplicate images are exactly the same as the ones at the origin $z = 0$. More importantly, at the fraction of the Talbot distance and if we choose $z = Z_T/N$, there are N-fold duplicate images of the original one. The spatial coefficient can be expressed equivalently as

$$a = \frac{d^2}{Z_T/z} = \frac{d^2}{N}. \tag{6}$$

Intuitively, if the spatial coefficient a is substituted by $1/\alpha$, and the distance d by T, we have

$$\alpha = N/T^2\,. \tag{7}$$

In (7), the chirp rate α is thus related to the critical condition of the Talbot effect where duplicated images are formed. In Fig. 2 (b), the Talbot images at a fraction of the Talbot distance, i.e., z

This article has been accepted for publication in a future issue of this journal, but has not been fully edited. Content may change prior to final publication. Citation information: DOI 10.1109/LSP.2017.2737596, IEEE Signal Processing Letters

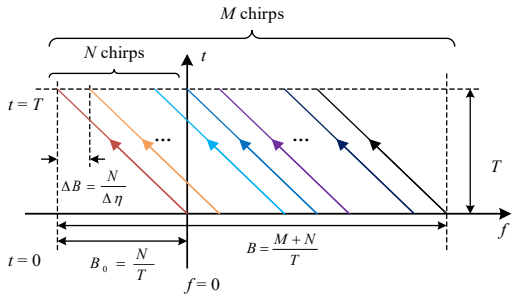

Fig. 3. Illustration of the spectrogram of a family of M orthogonal chirps with period T under the orthogonality condition with $\alpha = N/T^2$ and $\Delta\eta = T/N$.

$= Z_T/N$, are spaced by d/N. By analogy, a temporal shift can be defined by replacing d by T, as $\Delta\eta = T/N$.

With these results, a root chirped waveform is defined as

$$\psi_0(t) = \frac{1}{\sqrt{T}} e^{-j\frac{\pi}{4}} e^{-j\pi\frac{N}{T^2}t^2}, \quad 0 \le t < T, \tag{8}$$

and a family of M mutually orthogonal linear chirps, $\psi_k(t)$, can be defined by shifting the root chirp at integers of $\Delta\eta$, as

$$\psi_k(t) = \psi_0(t - k\Delta\eta) = \frac{1}{\sqrt{T}} e^{-j\frac{\pi}{4}} e^{-j\pi\frac{N}{T^2}\left(t-k\frac{T}{N}\right)^2}, \quad 0 \le t < T, \tag{9}$$

where $k = 0, 1, \ldots, M-1$. It can be easily proved that for any $\psi_k(t)$ and $\psi_m(t)$, we have

$$\int \psi_m^*(t)\psi_k(t)\mathrm{d}t = \delta(m-k), \tag{10}$$

where $\delta(k)$ is the Kronecker delta function.

Thus, we can make the following remarks: Given a period T, there is a family of M mutually orthogonal chirps as defined in (9) if the chirp rate $\alpha = N/T^2$ and the chirps are shifted in frequency at integer multiples of $\Delta\eta = 1/(\alpha T)$, where $N, M \in \mathbb{Z}^+$. Fig. 3 illustrates the spectrogram of this family of orthogonal chirps, with M being a positive integer independent of N.

B. Approaching the Nyquist Rate with the Orthogonal Chirps

It can be seen in Fig. 3 that the root chirp is a down-chirp and each chirp is linearly shifted at integer multiples of $\Delta\eta = T/N$ in the same direction. In fact, the sign of α can be altered to obtain a family of positively chirped waveforms. Regardless of the sign of α, the M orthogonal chirps occupy the same bandwidth.

For the family of M orthogonal chirps, as defined in (9), the occupied bandwidth is $B = (M+N)/T$ (Hz), the Baud rate is $R = 1/T$ (Baud/s), and the processing gain of the chirps is defined in terms of the time-bandwidth product $N = B_0 \times T$ (Hz·s), with B_0 as the bandwidth of a single chirp. The normalized modulation rate of the orthogonal chirps is thus

$$\beta = \frac{R}{B} = \frac{M}{M+N} \quad (\text{Baud/s/Hz}). \tag{11}$$

In Fig. 4, the normalized modulation rate in (11) is plotted as a function of M and N. It can be easily deduced that as M goes to infinity or is sufficiently larger than N,

$$\lim_{M\to+\infty} \beta = 1, \tag{12}$$

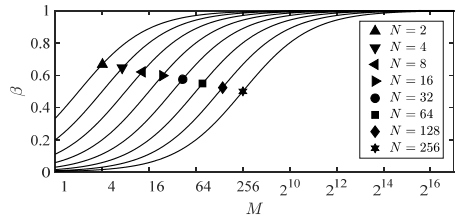

Fig. 4. Normalized modulation rate of the orthogonal chirps as a function of processing gain N for different number of chirps M.

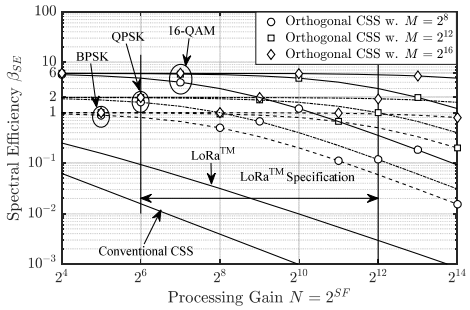

Fig. 5. Spectral efficiencies of conventional CSS, LoRa-CSS and the proposed orthogonal CSS versus processing gain.

which actually means the Nyquist rate.

In the conventional CSS that encodes information using up- and down-chirps, the spectral efficiency is inversely proportional to the processing gain, as $\beta_{SE\text{-}\Lambda} = 1/N$ (bit/s/Hz). On the other hand, modulation formats involving amplitude and phase modulation are not optimal due to the existence of interference [10]. Thus, in the LoRa-CSS, FSK is employed to modulate the quasi-orthogonal chirps to mitigate the interference and also to improve the spectral efficiency by a factor of $\log_2 N$ compared to the conventional CSS. Its spectral efficiency is $\beta_{SE\text{-LoRa}} = N^{-1}\log_2 N$ (bit/s/Hz), where $N = 2^{SF}$ is the processing gain, with $SF = 6$ to 12 being the spread factor [9].

In our proposed orthogonal CSS, with the orthogonal $\psi_k(t)$ in (9), spectrally efficient modulation formats, such as QAM, can be employed for high-speed communications. As the chirps are orthogonal, no interference exists among them. For example, if 2^κ-QAM with modulation order κ is employed, the spectral efficiency is $\beta_{SE\text{-}2^\kappa\text{-QAM}} = \kappa\beta$.

Fig. 5 compares the spectral efficiencies of the conventional CSS, LoRa-CSS and the proposed orthogonal CSS. It can be seen that LoRa-CSS improves spectral efficiency by a factor of $\log_2 N$ compared to the conventional CSS. Its spectral efficiency is still limited. In the orthogonal CSS, if modulation formats, such as BPSK, QPSK and 64-QAM (with $\kappa = 1, 2, 6$), are employed, the spectral efficiency approaches that of the Nyquist signaling by suitably adjusting M and N. Moreover, orthogonal signaling, such as FSK, can be employed in the proposed CSS for power-limited system by modulating the index of the chirps, and then the spectral efficiency will be similar to that of LoRa-CSS. In the next section, we will show that, due to the advantage of orthogonal (Nyquist) signaling, the proposed CSS exhibits better receiver sensitivity than the LoRa-CSS.

IV. Performance Analysis and Discussions

In this section, the performance of the proposed orthogonal CSS is analyzed considering both power and bandwidth limited

This article has been accepted for publication in a future issue of this journal, but has not been fully edited. Content may change prior to final publication. Citation information: DOI 10.1109/LSP.2017.2737596, IEEE Signal Processing Letters

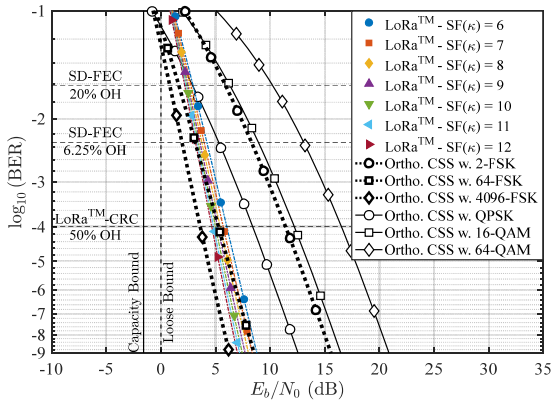

Fig. 6. Normalized modulation rate of the orthogonal chirps as a function of processing gain N for different number of chirps M.

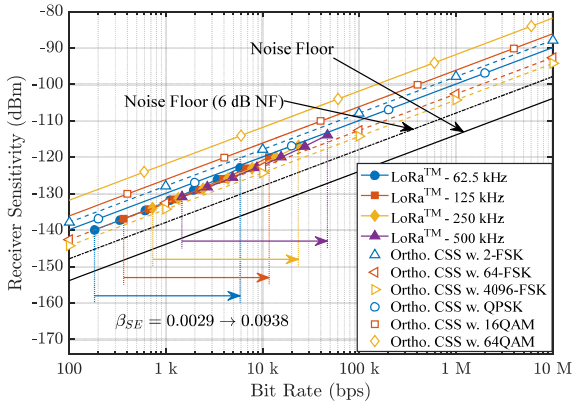

Fig. 7. Receiver sensitivities of LoRa-CSS and the proposed orthogonal CSS with FSK and QAM modulations versus bit rate.

systems for practical applications. On one hand, in the LPWAN systems with power constraint, bandwidth is traded for better receiver sensitivity. On the other hand, in the WLAN or cellular networks, spectrally efficient modulation formats such as QAM are a preferred choice for supporting a higher data rate within a given bandwidth.

In the IoT applications, for example, the power is limited to 14 dBm in the 868 MHz ISM-band and the transmission distance should cover several tens of km. Orthogonal signaling, such as FSK, can be employed for reliability. In the LoRa-CSS, as the chirps are quasi-orthogonal, although FSK is used, higher processing gain and coding gain are needed to compensate for the performance loss [10]. TABLE I lists the required demodulation signal-to-noise ratio (SNR) of LoRa™ system with 50% cyclic redundancy code overhead. The equivalent E_b/N_0 is also calculated as reference in TABLE I, and it can be seen that 5 dB is the equivalent demodulation SNR per bit [9].

In Fig. 6, the BER performance of LoRa-CSS under additive white Gaussian noise (AWGN) is calculated with respect to E_b/N_0 based on the results in [10]. It can be seen that $E_b/N_0 = 5$ dB corresponds to a BER = 10^{-4}. The soft-decision FEC limits with 6.25% and 20% overhead are shown in Fig. 6 for comparison [18]. The BER performance of the proposed CSS with FSK is also evaluated against AWGN. At BER = 10^{-4}, the orthogonal CSS with FSK achieves about 0.5 and 1 dB improvement over LoRa-CSS for $\kappa = 6$ and 12, respectively. The improvement is because the chirps in (9) are orthogonal while those of LoRa-CSS are not. According to the Shannon's theory, the capacity bound of the proposed CSS with FSK is −1.59 dB, as plotted on the left-most side in Fig. 6 [19]. The loose bound for LoRa-CSS calculated from (21) in [10] is next to it. In Fig. 6, the BER performance of the proposed CSS with QPSK, 16-QAM, and 64-QAM is also provided. In contrast to FSK, the performance degrades as κ increases but their spectral efficiency improves significantly.

TABLE I
REQUIRED DEMODULATION SNR IN LORA™

	Processing Gain $N = 2^{SF}$						
SF	**6**	**7**	**8**	**9**	**10**	**11**	**12**
SNR (dB)	−5.0	−7.5	−10.0	−12.5	−15.0	−17.5	−20.0
E_b/N_0 (dB)	5.28	5.12	5.05	5.05	5.10	5.20	5.33

Note: The parameters are obtained from the datasheet of the Semtech LoRa™ SX1276/77/78/79 module.

Based on the performance in Fig. 6, the receiver sensitivities of LoRa-CSS with different spreading factors to achieve a BER = 10^{-4} are shown in Fig. 7, by considering thermal noise with power density −174 dBm/Hz at 300 K. It should be noted that in Fig. 7, a 6-dB amplifier noise figure is also taken into account. In the LoRa-CSS, as the bandwidths are fixed at 62.5, 125, 250, and 500 kHz, the bit rate is changed by varying the spreading factor from 6 to 12. The receiver sensitivities of the proposed orthogonal CSS with 2-FSK (κ = 1), 64-FSK (κ = 6) and 4096-FSK (κ = 12) are provided for comparison. It can be seen that the proposed CSS with FSK achieves 1-dB sensitivity improvement over the LoRa-CSS under the same conditions.

In addition, the receiver sensitivities of the proposed CSS with QPSK, 16-QAM and 64-QAM are provided for comparison. Although the receiver sensitivities degrade with about 2, 6, and 11 dBm, respectively, their spectral efficiencies are 2, 4, and 6 (bit/s/Hz), which are much greater than that of LoRa-CSS which are usually less than 0.1. In the LTE system for example, highly spectrally efficient modulation formats are the inevitable choice. In theory, the proposed CSS has similar performance as the OFDM system as orthogonality holds for both of them. Moreover, as spread spectrum is enabled in the proposed CSS, potential utilization of multipath diversity is possible by adjusting the processing gain of the chirps, and thus with potential performance improvement over multipath fading channels.

V. CONCLUSION

In this letter, the orthogonality condition for multiplexing an arbitrary number of orthogonal chirps is derived and presented for CSS system to achieve the Nyquist signaling rate. According to this condition, the processing gain of the chirps can be set independently with respect to the number of orthogonal chirps. The design of orthogonal CSS is thus more flexible for various applications. It is also shown that for power-limited applications such as IoT, the proposed orthogonal CSS outperforms LoRa-CSS by virtue of such orthogonality. Moreover, spectrally efficient modulation formats can be employed with the proposed CSS to support high data rate communications.

REFERENCES

[1] E. Karapistoli, F. N. Pavlidou, I. Gragopoulos *et al.*, "An overview of the IEEE 802.15.4a standard," *IEEE Commun. Mag.,* vol. 48, pp. 47-53, Jan. 2010.

[2] C. Goursaud and J.-M. Gorce, "Dedicated networks for IoT: PHY/MAC state of the art and challenges," *EAI Endorsed Transactions on Internet of Things,* vol. 1, pp. 1-11, Oct. 2015.

[3] M. Centenaro, L. Vangelista, A. Zanella *et al.*, "Long-range communications in unlicensed bands: the rising stars in the IoT and smart city scenarios," *IEEE Wirel. Commun.,* vol. 23, pp. 60-67, Nov. 2016.

[4] "IEEE Standard for Low-Rate Wireless Networks," in *IEEE Std 802.15.4-2015 (Revision of IEEE Std 802.15.4-2011)*, ed, 2016, pp. 1-709.

[5] S. E. El-Khamy and S. E. Shaaban, "Matched chirp modulation: detection and performance in dispersive communication channels," *IEEE Trans. Commun.,* vol. 36, pp. 506-509, Apr. 1988.

[6] H. Bush, A. Martin, R. F. Cobb *et al.*, "Application of chirp SWD for spread spectrum communications," in *Proc. 1973 Ultrasonics Symposium*, 1973, pp. 494-497.

[7] M. Kowatsch and J. Lafferl, "A spread-spectrum concept combining chirp modulation and pseudonoise coding," *IEEE Trans. Commun.,* vol. 31, pp. 1133-1142, Jan. 1983.

[8] H. P. Liu, "Multicode ultra-wideband scheme using chirp waveforms," *IEEE J. Sel. Areas Commun.,* vol. 24, pp. 885-891, Apr. 2006.

[9] "SX1276/77/78/79 - 137 MHz to 1020 MHz Low Power Long Range Transceiver," Semtech Corporation, Datasheet SX1276/77/78/79, August 2016.

[10] B. Reynders and S. Pollin, "Chirp spread spectrum as a modulation technique for long range communication," in *Proc. Symposium on Communications and Vehicular Technologies (SCVT)*, Mons, Belgium, 2016, pp. 1-5.

[11] X. Ouyang and J. Zhao, "Orthogonal chirp division multiplexing," *IEEE Trans. Commun.,* vol. 64, pp. 3946-3957, Jul. 2016.

[12] X. Ouyang and J. Zhao, "Orthogonal chirp division multiplexing for coherent optical fiber communications," *J. Lightw. Technol.,* vol. 34, pp. 4376-4386, Aug. 2016.

[13] Xing Ouyang, Cleitus Antony, F. C. G. Gunning *et al.*, "Discrete Fresnel transform and its circular convolution property," *arXiv.org,* vol. arXiv:1510.00574, 2015.

[14] X. Ouyang, O. A. Dobre, and J. Zhao, "Unbiased Channel Estimation Based on the Discrete Fresnel Transform for CO-OFDM Systems," *IEEE Photon. Technol. Lett.,* vol. 29, pp. 691-694, 2017.

[15] M. Abramowitz, *Handbook of Mathematical Functions, with Formulas, Graphs, and Mathematical Tables*. Dover Publications, Incorporated, 1974.

[16] L. Rayleigh, "On copying diffraction-gratings, and on some phenomena connected therewith," *Philosophical Magazine Series 5,* vol. 11, pp. 196-205, Mar. 1881.

[17] J. T. Winthrop and C. R. Worthing, "Theory of Fresnel images .I. plane periodic objects in monochromatic light," *Journal of the Optical Society of America,* vol. 55, pp. 373-381, Apr. 1965.

[18] L. M. Zhang and F. R. Kschischang, "Staircase codes with 6% to 33% overhead," *J. Lightw. Technol.,* vol. 32, pp. 1999-2002, Apr. 2014.

[19] J. Proakis and M. Salehi, *Digital Communications*. 5th ed., New York, NY, USA: McGraw-Hill Education, 2007.